Reflection coefficients in attenuative anisotropic media

Jyoti Behura[1] and Ilya Tsvankin[2]

ABSTRACT

Such reservoir rocks as tar sands are characterized by significant attenuation and, in some cases, attenuation anisotropy. Most existing attenuation studies are focused on plane-wave attenuation coefficients, which determine the amplitude decay along the raypath of seismic waves. Here we study the influence of attenuation on PP- and PS-wave reflection coefficients for anisotropic media with the main emphasis on transversely isotropic models with a vertical symmetry axis (VTI). Concise analytic solutions obtained by linearizing the exact plane-wave reflection coefficients are verified by numerical modeling. To make a substantial contribution to reflection coefficients, attenuation must be strong, with the quality factor Q not exceeding 10. For such highly attenuative media, it is also necessary to take attenuation anisotropy into account if the magnitude of the Thomsen-style attenuation-anisotropy parameters is relatively large. In general, the linearized reflection coefficients in attenuative media include velocity-anisotropy parameters but have almost "isotropic" dependence on attenuation. Our formalism also helps evaluate the influence of the inhomogeneity angle (the angle between the real and imaginary parts of the slowness vector) on the reflection coefficients. A nonzero inhomogeneity angle of the incident wave introduces additional terms into the PP- and PS-wave reflection coefficients, which makes conventional amplitude-variation-with-offset (AVO) analysis inadequate for strongly attenuative media. For instance, an incident P-wave with a nonzero inhomogeneity angle generates a mode-converted PS-wave at normal incidence, even if both half-spaces have a horizontal symmetry plane. The developed linearized solutions can be used in AVO inversion for highly attenuative (e.g., gas-sand and heavy-oil) reservoirs.

INTRODUCTION

Conventional amplitude-variation-with-offset (AVO) analysis is carried out under the assumption that the subsurface is purely elastic. However, direct measurements using vertical seismic profiling (VSP) (Hauge, 1981; Hedlin et al., 2001), well logs (Schmitt, 1999), and rock samples (Behura et al., 2007; Winkler and Nur, 1982) show that attenuation (and, sometimes, velocity dispersion) can be significant, especially within hydrocarbon-saturated zones. Luh (1988) and Samec et al. (1990) attribute some failures of AVO analysis to the influence of attenuation. Furthermore, physical-modeling experiments (Hosten et al., 1987; Maultzsch et al., 2003; Zhu et al., 2007), rock-physics studies (Behura et al., 2006; Prasad and Nur, 2003; Tao and King, 1990), and analysis of field data (Liu et al., 1993; Lynn et al., 1999; Vasconcelos and Jenner, 2005) indicate that attenuation can be directionally dependent, with attenuation anisotropy being stronger than velocity anisotropy (Arts and Rasolofosaon, 1992; Hosten et al., 1987; Zhu et al., 2007).

Although most attenuation studies are focused on attenuation coefficients, which determine the amplitude decay along the raypath of seismic waves, it is also important to evaluate the influence of attenuation and attenuation anisotropy on plane-wave reflection/transmission coefficients. Reflection coefficients for a boundary between isotropic attenuative half-spaces have been studied analytically (Krebes, 1983; Ursin and Stovas, 2002) and using numerical modeling (Nechtschein and Hron, 1997; Hearn and Krebes, 1990). Sidler and Carcione (2007) and Stovas and Ursin (2003) discuss the influence of anisotropy on reflection/transmission coefficients in attenuative VTI media. Existing results for anisotropic models, however, do not provide physical insight into the dependence of plane-wave reflectivity on the medium properties, in particular on the anisotropy parameters that govern both velocity and attenuation.

Here, we develop linearized approximations for PP- and PS-wave

reflection coefficients at a boundary between arbitrarily anisotropic, attenuative half-spaces. Then the general solutions are simplified for vertical transverse isotropy and expressed through the Thomsen-style parameters introduced by Zhu and Tsvankin (2006). It should be emphasized that our formalism takes into account the inhomogeneity angle (the angle between the real and imaginary parts of the slowness vector) of the incident wave. Finally, we compute exact reflection coefficients for a realistic range of the velocity- and attenuation-anisotropy parameters and assess the accuracy of the linearized expressions.

PERTURBATION ANALYSIS OF REFLECTION/TRANSMISSION COEFFICIENTS

For a welded contact between two arbitrarily anisotropic, attenuative half-spaces, the boundary conditions of the continuity of traction and displacement result in the following system of six linear equations (e.g., Vavryčuk and Pšenčík, 1998):

$$\widetilde{\mathbf{C}}\,\widetilde{\mathbf{U}} = \widetilde{\mathbf{B}}, \tag{1}$$

where the tilde denotes a complex quantity, $\widetilde{\mathbf{C}}$ corresponds to the displacement-stress matrix for the reflected and transmitted plane waves P, S_1, and S_2, $\widetilde{\mathbf{B}}$ is the displacement-stress vector of the incident wave, and $\widetilde{\mathbf{U}}$ is the vector of the reflection (R) and transmission (T) coefficients. The matrix $\widetilde{\mathbf{C}}$ and the vectors $\widetilde{\mathbf{U}}$ and $\widetilde{\mathbf{B}}$ are composed of complex elements because the stiffness tensor in attenuative media is complex. Exact reflection/transmission coefficients ($\widetilde{\mathbf{U}}$) can be computed by solving the system of equations 1 numerically.

Following Vavryčuk and Pšenčík (1998) and Jílek (2002a, 2002b), we apply the first-order perturbation theory to a background homogeneous medium, which is taken to be isotropic and attenuative. Linearization of the boundary conditions (equation 1) yields the perturbation $\delta\widetilde{\mathbf{U}}$ in the form

$$\delta\widetilde{\mathbf{U}} = (\widetilde{\mathbf{C}}^0)^{-1}(\delta\widetilde{\mathbf{B}} - \delta\widetilde{\mathbf{C}}\,\widetilde{\mathbf{U}}^0). \tag{2}$$

Here, $\widetilde{\mathbf{C}}^0$ is the displacement-stress matrix for the reflected/transmitted waves in the background medium and $\delta\widetilde{\mathbf{C}}$ represents the perturbation of $\widetilde{\mathbf{C}}^0$. Similarly, $\delta\widetilde{\mathbf{B}}$ is the perturbation of the displacement-stress vector of the incident wave. The vector of the amplitudes of the reflected and transmitted waves in the homogeneous background $\widetilde{\mathbf{U}}^0$ is given by
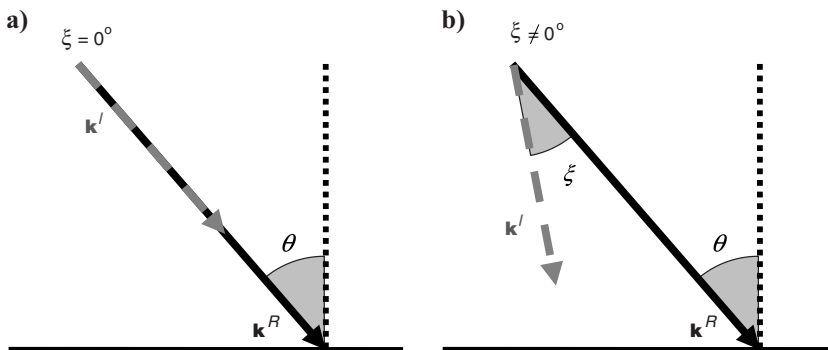

Figure 1. Incident plane wave with (a) zero inhomogeneity angle and (b) nonzero inhomogeneity angle ξ. The vectors $\mathbf{k}^R$ and $\mathbf{k}^I$ are the real and imaginary components (respectively) of the wave vector, and θ is the incidence phase angle.

$$\widetilde{\mathbf{U}}^0 = [0,\,0,\,0,0,\,0,\,1]^T; \tag{3}$$

the only nonzero term in equation 3 represents the P-wave transmission coefficient.

Ursin and Stovas (2002) adopt a similar perturbation approach to derive reflection/transmission coefficients for isotropic attenuative media. (Their formalism introduces a weak contrast in the parameters across the interface while keeping both half-spaces isotropic.) The change in the slownesses and polarizations of the scattered waves, required for obtaining $\delta\widetilde{\mathbf{C}}$ and $\delta\widetilde{\mathbf{B}}$ in equation 2, can be computed by perturbing the isotropic background medium (Jech and Pšenčík, 1989). We extend this method, developed for purely elastic media, to attenuative models by taking the background attenuation into account.

The density-normalized complex stiffness tensor $\widetilde{a}_{ijkl}$ of the perturbed medium can be written as

$$\widetilde{a}_{ijkl} = \widetilde{a}^0_{ijkl} + \delta\widetilde{a}_{ijkl}, \tag{4}$$

where the tensor $\widetilde{a}^0_{ijkl} = a^0_{ijkl} + ia^{0,I}_{ijkl}$ corresponds to the background medium, and the perturbation $\delta\widetilde{a}_{ijkl}$ is responsible for both the velocity and attenuation anisotropy of the perturbed medium.

The quality-factor (Q) matrix (in the two-index Voigt notation) is defined as (e.g., Carcione, 2007)

$$Q_{ij} = \frac{a^R_{ij}}{a^I_{ij}}. \tag{5}$$

For isotropic media, the Q-matrix takes the form

$$Q = \begin{bmatrix} Q_{P0} & Q_{13} & Q_{13} & 0 & 0 & 0 \\ Q_{13} & Q_{P0} & Q_{13} & 0 & 0 & 0 \\ Q_{13} & Q_{13} & Q_{P0} & 0 & 0 & 0 \\ 0 & 0 & 0 & Q_{S0} & 0 & 0 \\ 0 & 0 & 0 & 0 & Q_{S0} & 0 \\ 0 & 0 & 0 & 0 & 0 & Q_{S0} \end{bmatrix}, \tag{6}$$

where Q_{P0} and Q_{S0} control the P- and the S-wave attenuation, respectively, and Q_{13} is the following function of Q_{P0} and Q_{S0} (Zhu and Tsvankin, 2006):

$$Q_{13} = Q_{P0}\frac{a_{33} - 2a_{55}}{a_{33} - 2a_{55}\dfrac{Q_{P0}}{Q_{S0}}}. \tag{7}$$

If the medium is attenuative, the wave vector becomes complex, and its real ($\mathbf{k}^R$) and imaginary ($\mathbf{k}^I$) parts might have different orientations. The angle ξ between $\mathbf{k}^R$ and $\mathbf{k}^I$ usually is called the inhomogeneity angle (Figure 1b). For $\xi = 0°$ (so-called "homogeneous wave propagation," Figure 1a), the phase direction coincides with the direction of maximum attenuation.

Plane-wave propagation in anisotropic media is described by the Christoffel equation, which can be solved for the phase velocity, polarization vector, and phase attenuation coefficient. The Christoffel equation for a zero inhomogeneity angle can be written as

$$(\widetilde{a}_{ijkl}\widetilde{k}^2 n_i n_l - \omega \delta_{jk})\widetilde{u}_j = 0, \qquad (8)$$

where **n** is the unit slowness vector, ω is the frequency, $\widetilde{\mathbf{u}}$ is the polarization vector, and

$$\widetilde{k} = k^R - ik^I; \qquad (9)$$

$k^R = |\mathbf{k}^R|$ controls the phase velocity and $k^I = |\mathbf{k}^I|$ is responsible for the phase attenuation. The ratio of k^I and k^R defines the normalized attenuation coefficient $\mathcal{A}$, which yields the rate of amplitude decay per wavelength (Zhu and Tsvankin, 2006):

$$\mathcal{A} = \frac{k^I}{k^R}. \qquad (10)$$

When attenuation is weak or moderate $(1/Q \ll 1)$ and isotropic,

$$\mathcal{A} \approx \frac{1}{2Q}. \qquad (11)$$

The perturbations of the wave $(\delta\widetilde{\mathbf{k}})$ and polarization $(\delta\widetilde{\mathbf{u}})$ vectors, obtained by substituting the perturbed tensor $\widetilde{a}_{ijkl}$ (equation 4) into the Christoffel equation 8, are used in equation 2 to derive the perturbation $\delta\widetilde{\mathbf{U}}$ of the reflection/transmission coefficients (Jech and Pšenčík, 1989; Vavryčuk and Pšenčík, 1998; Jílek, 2002b). Note that the perturbation analysis based on equation 8 is strictly valid only for plane waves with a zero inhomogeneity angle ξ. Nevertheless, as shown below, our results can be extended in a straightforward way to waves with moderate angles ξ, even if the model has strong attenuation with $Q < 10$.

The complex P- and S-wave velocities $(\widetilde{V}_{P0}$ and $\widetilde{V}_{S0})$ in the background attenuative isotropic medium have the form

$$\widetilde{V}_{P0} = \frac{\omega}{\widetilde{k}_{P0}} \approx V_{P0}(1 + i\mathcal{A}_{P0}), \qquad (12)$$

$$\widetilde{V}_{S0} = \frac{\omega}{\widetilde{k}_{S0}} \approx V_{S0}(1 + i\mathcal{A}_{S0}), \qquad (13)$$

where V_{P0} and V_{S0} are the phase velocities of P- and S-waves, respectively, and $\mathcal{A}_{P0}$ and $\mathcal{A}_{S0}$ are the corresponding normalized attenuation coefficients. In equations 12 and 13, terms of the second and higher order in $1/Q$ are neglected.

INCIDENT P-WAVE WITH A ZERO INHOMOGENEITY ANGLE

If the angle ξ is set to zero, all terms in equation 2 coincide with those given in Vavryčuk and Pšenčík (1998) and Jílek (2002a, 2002b) for nonattenuative media, but they become complex quantities. Hence, the linearized reflection coefficients for P-waves (Vavryčuk and Pšenčík, 1998) and PS-waves (Jílek, 2002a) can be adapted in a straightforward way for attenuative media.

PP-wave reflection coefficient

Arbitrarily anisotropic media

The linearized PP-wave reflection coefficient in arbitrarily anisotropic media obtained from equation 2 is given by

$$R_{PP}^{H} = \frac{\Delta\rho}{2\rho_0} + \frac{\Delta\widetilde{a}_{33}}{4\widetilde{V}_{P0}^2} + \left(\frac{\Delta\widetilde{a}_{13}}{2\widetilde{V}_{P0}^2} - \frac{\Delta\widetilde{a}_{33}}{4\widetilde{V}_{P0}^2} - \frac{\Delta\widetilde{a}_{55}}{\widetilde{V}_{P0}^2} \right.$$
$$\left. - \frac{2\widetilde{V}_{S0}^2}{\widetilde{V}_{P0}^2}\frac{\Delta\rho}{\rho_0} \right)\sin^2\theta + \frac{\Delta\widetilde{a}_{11}}{4\widetilde{V}_{P0}^2}\sin^2\theta \tan^2\theta, \quad (14)$$

where the superscript H (homogeneous) indicates that the incident wave has a zero inhomogeneity angle, Δ is the contrast in a certain parameter across the interface, ρ_0 is the density of the background medium, $\widetilde{a}_{ij}$ are the density-normalized complex stiffness coefficients in Voigt notation (i.e., the stiffness matrix), and θ is the incidence angle (Figure 1a).

Equation 14 is derived under the assumption that the contrasts in the medium properties across the interface are small $(|\Delta\widetilde{a}_{ijkl}| \ll \|\widetilde{a}_{ijkl}^0\|, |\Delta\rho| \ll \rho^0, \widetilde{a}_{ijkl}^0$ and ρ^0 are the background stiffness tensor and density). The linearized reflection coefficient in equation 14 reduces to that in purely elastic media, if all complex quantities are made real. Although equation 14 is strictly valid only if all waves have a zero inhomogeneity angle, it remains sufficiently accurate for a wide range of ξ values, unless the medium is strongly attenuative (see below).

VTI media

Next we analyze equation 14 for the special case of attenuative VTI media using Thomsen-style notation. In addition to the well-known Thomsen velocity parameters V_{P0}, V_{S0}, ϵ, δ, and γ, we employ the attenuation parameters $\mathcal{A}_{P0}$, $\mathcal{A}_{S0}$, ϵ_Q, δ_Q, and γ_Q introduced by Zhu and Tsvankin (2006). $\mathcal{A}_{P0} \approx 1/(2Q_{P0})$ and $\mathcal{A}_{S0} \approx 1/(2Q_{S0})$ are the normalized symmetry-direction (vertical) attenuation coefficients of P- and S-waves, respectively, ε_Q and δ_Q control the angular variation of the P- and SV-wave attenuation coefficients, and γ_Q governs SH-wave attenuation anisotropy.

To simplify the reflection coefficient, it is convenient to assume that terms proportional to $1/Q_{P0}^2$ and $1/Q_{S0}^2$ are sufficiently small to be dropped. Then equation 14 takes the form

$$R_{PP}^{H} = R_{PP}^{H}(0) + G_{PP}^{H}\sin^2\theta + C_{PP}^{H}\sin^2\theta \tan^2\theta, \quad (15)$$

where $R_{PP}^{H}(0)$ is the normal-incidence PP-wave reflection coefficient (AVO intercept), G_{PP}^{H} is the AVO gradient, and C_{PP}^{H} is the curvature term. Equation 15 is a Shuey-type approximation for the PP reflection coefficient in attenuative media, in which all three terms are complex:

$$R_{PP}^{H}(0) = \frac{\Delta\rho}{2\rho_0} + \frac{\Delta V_{P0}}{2V_{P0}} + \frac{\Delta\mathcal{A}_{P0}}{2}\left(i + \frac{1}{Q_{P0}} \right), \quad (16)$$

$$G_{PP}^{H} = \frac{-2}{g^2}\frac{\Delta\rho}{\rho_0} + \frac{\Delta V_{P0}}{2V_{P0}} - \frac{4}{g^2}\frac{\Delta V_{S0}}{V_{S0}} + \frac{\Delta\delta}{2} + i\left(\frac{\Delta\mathcal{A}_{P0}}{2} \right.$$
$$\left. - \frac{4\Delta\mathcal{A}_{S0}}{g^2} \right) + \frac{i}{Q_{P0}}\left(\frac{2}{g^2}\frac{\Delta\rho}{\rho_0} + \frac{4}{g^2}\frac{\Delta V_{S0}}{V_{S0}} - \frac{i}{2}\Delta\mathcal{A}_{P0} \right.$$
$$\left. + \frac{4i}{g^2}\Delta\mathcal{A}_{S0} + \frac{\Delta\delta_Q}{4} \right) - \frac{i}{Q_{S0}}\frac{2}{g^2}\left(\frac{\Delta\rho}{\rho_0} + 2\frac{\Delta V_{S0}}{V_{S0}} \right),$$
$$(17)$$

and

$$C_{\mathrm{PP}}^{\mathrm{H}} = \frac{\Delta V_{\mathrm{P0}}}{2 V_{\mathrm{P0}}} + \frac{\Delta \varepsilon}{2} + \frac{i}{2} \Delta \mathcal{A}_{\mathrm{P0}} + \frac{1}{Q_{\mathrm{P0}}} \left(\frac{\Delta \mathcal{A}_{\mathrm{P0}}}{2} + \frac{i}{4} \Delta \varepsilon_Q \right);$$

(18)

$$g \equiv V_{\mathrm{P0}} / V_{\mathrm{S0}}.$$

Eliminating the influence of attenuation on $R_{\mathrm{PP}}^{\mathrm{H}}(0)$, $G_{\mathrm{PP}}^{\mathrm{H}}$, and $C_{\mathrm{PP}}^{\mathrm{H}}$ in equations 16–18 reduces them to the expressions for the PP-wave intercept, gradient, and curvature (respectively) for purely elastic VTI media (Rüger, 2002). As illustrated by Figure 2, the linearized approximation stays close to the exact reflection coefficient for a wide range of θ values, even when Q_{P0} is as low as 10. The decrease in the accuracy of equation 15 with incidence angle (Figure 2) is typical for weak-contrast, weak-anisotropy approximations for reflection coefficients.

Because the attenuation coefficient $\mathcal{A} \sim 1/(2Q)$, it is clear from equations 16–18 that the influence of attenuation on the reflection coefficient is comparable to that of the velocity and density contrasts only if the quality factor is small (e.g., Q_{P0}, $Q_{S0} < 10$). This conclusion is confirmed by the test in Figure 3 with the model parameters simulating an interface between purely elastic shale and attenuative oil sand. When the attenuation in the sand is moderate ($Q_{P,2} = 2Q_{S,2} = 50$), the coefficient $R_{\mathrm{PP}}^{\mathrm{H}}$ is almost identical to that in the elastic
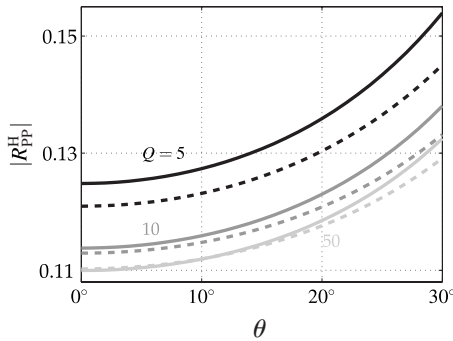

Figure 2. Magnitude of the PP-wave reflection coefficient at the ocean floor for different values of the quality factor Q of the ocean-floor sediments ($Q = Q_{\mathrm{P0,2}} = 2Q_{\mathrm{S0,2}}$). The solid lines are the exact coefficients; the dashed lines mark the linearized approximation 15. The model parameters are listed in Table 1.
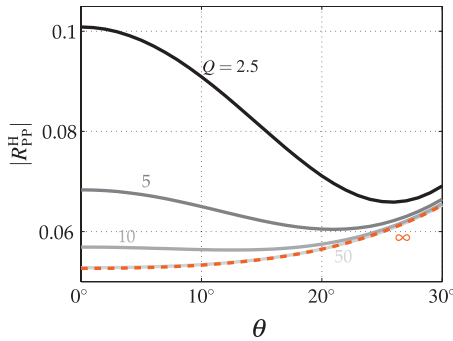

Figure 3. Magnitude of the exact PP-wave reflection coefficient for an interface between VTI shale with negligible attenuation and attenuative isotropic oil sand (Table 1). The solid lines correspond to different Q-values in the sand ($Q = Q_{\mathrm{P0,2}} = 2Q_{\mathrm{S0,2}}$); the dashed line corresponds to zero attenuation ($Q_{\mathrm{P0,2}} = Q_{\mathrm{S0,2}} = \infty$).

case. Even a small Q-value of 10 does not noticeably change the reflection coefficient. However, when the attenuation is extremely strong ($Q_{P,2} = 2Q_{S,2} = 2.5$ or 5), the reflection coefficient substantially deviates from that for the purely elastic model.

The "isotropic" parameter $\Delta \mathcal{A}_{\mathrm{P0}}$ in equation 16 is responsible for the influence of attenuation on the normal-incidence reflection coefficient. In addition, $\Delta \mathcal{A}_{\mathrm{P0}}$ makes a more significant contribution to $G_{\mathrm{PP}}^{\mathrm{H}}$ and $C_{\mathrm{PP}}^{\mathrm{H}}$ than do ε_Q and δ_Q because the attenuation-anisotropy parameters in equations 17 and 18 are scaled by $1/Q_{\mathrm{P0}}$. In general, the contribution of the terms multiplied with $1/Q_{\mathrm{P0}}$ and $1/Q_{\mathrm{S0}}$ in equations 16–18 is of the second order, unless the medium has extremely high attenuation.

As is the case for purely elastic VTI media, the linearized P-wave AVO gradient (equation 17) is sensitive to the velocity-anisotropy parameter δ. Although the attenuation-anisotropy parameter δ_Q governs the P-wave attenuation near the symmetry axis, the scaling factor $1/Q_{\mathrm{P0}}$ makes its influence on $G_{\mathrm{PP}}^{\mathrm{H}}$ less significant than that of δ. Similarly, the curvature term $C_{\mathrm{PP}}^{\mathrm{H}}$ (equation 18) is more sensitive to the parameter ϵ than to ε_Q (note that ε_Q does not contribute to the linearized AVO gradient). The parameters γ and γ_Q control only the anisotropy of SH-waves, which are decoupled from P- and SV-waves analyzed here. On the whole, the reflection coefficient for typical subsurface formations with $Q > 10$ is more sensitive to velocity anisotropy than to attenuation anisotropy.

The influence of the parameter δ_Q on the AVO gradient is illustrated in Figure 4 where the model is similar to that in Figure 3, but the oil sand (reflecting medium) exhibits attenuation anisotropy. When attenuation is weak ($Q = 50$), the AVO gradient barely varies with

Table 1. Medium parameters used in the numerical tests. For all models, the symmetry-direction velocities (V_{P0} and V_{S0}) are in km/s and density (ρ) is in gm/cm³. A dash means that the parameter value is shown on the plot.

Parameters	Fig. 2	Fig. 3	Fig. 4	Figs. 5 and 6	Fig. 8	Fig. 9
ρ_1	1.0	2.0	2.0	2.0	2.3	2.3
$V_{\mathrm{P0,1}}$	1.5	2.0	2.0	2.0	3.3	3.3
$V_{\mathrm{S0,1}}$	0	1.1	1.1	1.1	1.9	1.9
δ_1	0	0.2	0.2	0.2	0	0
ϵ_1	0	0.1	0.1	0.1	0	0
$Q_{\mathrm{P0,1}}$	∞	500	500	—	5	—
$Q_{\mathrm{S0,1}}$	∞	250	250	—	2.5	—
$\delta_{Q,1}$	0	0.8	0.8	0.8	0	0
$\epsilon_{Q,1}$	0	-0.4	-0.4	-0.4	0	0
ρ_2	1.1	2.0	2.0	2.0	2.0	2.0
$V_{\mathrm{P0,2}}$	1.7	1.8	1.8	1.8	2.5	2.5
$V_{\mathrm{S0,2}}$	0.1	1.0	1.0	1.0	1.3	1.3
δ_2	0	0	0	0	0	0.1
ϵ_2	0	0	0	0	0	0.2
$Q_{\mathrm{P0,2}}$	—	—	—	—	10	—
$Q_{\mathrm{S0,2}}$	—	—	—	—	5	—
$\delta_{Q,2}$	0	0	—	0	0	0.8
$\epsilon_{Q,2}$	0	0	0	0	0	-0.4

δ_Q. However, as the magnitude of attenuation increases ($Q \lesssim 10$), the influence of attenuation anisotropy becomes pronounced; strong attenuation can even change the sign of the AVO gradient. Our results confirm the common view that moderate attenuation does not substantially distort reflection coefficients. For highly attenuative media with $Q < 10$, however, it is necessary to consider not just attenuation, but also attenuation anisotropy.

PS-wave reflection coefficient for VTI media

Using the approach outlined above, we obtained the following closed-form linearized expression for the PS-wave reflection (conversion) coefficient in attenuative VTI media:

$$R_{\text{PS}}^{\text{H}} = B_{\text{PS}}^{\text{H}} \sin\theta + K_{\text{PS}}^{\text{H}} \sin^3\theta, \tag{19}$$

where the coefficients B_{PS}^{H} and K_{PS}^{H} (the gradient and curvature terms, respectively, in conventional PS-wave AVO analysis) are given by

$$B_{\text{PS}}^{\text{H}} = -\frac{2+g}{2g}\frac{\Delta\rho}{\rho_0} - \frac{2}{g}\frac{\Delta V_{\text{S0}}}{V_{\text{S0}}} + \frac{g}{2(1+g)}\Delta\delta - i\frac{2}{g}\Delta\mathcal{A}_{\text{S0}}$$
$$+ \frac{i}{Q_{\text{P0}}}f_1 - \frac{i}{Q_{\text{S0}}}f_2, \tag{20}$$

$$K_{\text{PS}}^{\text{H}} = \frac{(3+2g)}{4g^2}\frac{\Delta\rho}{\rho_0} + \frac{2+g}{g^2}\frac{\Delta V_{\text{S0}}}{V_{\text{S0}}} + \frac{1-4g}{2(1+g)}\Delta\delta$$
$$+ \frac{g}{1+g}\Delta\varepsilon + i\frac{2+g}{g^2}\Delta\mathcal{A}_{\text{S0}} - \frac{i}{2Q_{\text{P0}}}f_3 + \frac{i}{2Q_{\text{S0}}}f_4. \tag{21}$$

Here, f_1, f_2, f_3, and f_4 are linear combinations of the parameter contrasts across the interface listed in Appendix A. The contributions of $f_{1,2,3,4}$ to the reflection coefficient are of the second order because these functions are scaled by $1/Q_{\text{P0}}$ or $1/Q_{\text{S0}}$.

The real part of the reflection coefficient in equation 19 coincides with the corresponding linearized expression for PS-waves in a purely elastic VTI medium. Most conclusions drawn above for PP-waves remain valid for the PS-wave reflection coefficient as well. In particular, the influence of the attenuation contrasts on R_{PS}^{H} becomes comparable to that of the velocity and density contrasts only when $Q_{\text{P0}}, Q_{\text{S0}} < 10$. The attenuation-related part of R_{PS}^{H} is controlled primarily by the contrast in the vertical S-wave attenuation coefficient $\mathcal{A}_{\text{S0}}$ because $\Delta\epsilon_Q$ and $\Delta\delta_Q$ contribute only to the functions $f_{1,3}$ multiplied with $1/Q_{\text{P0}}$ (equations A-1 and A-3).

INCIDENT P-WAVE WITH A NONZERO INHOMOGENEITY ANGLE

If the upper half-space is attenuative, the incident P-wave can have a nonzero inhomogeneity angle ξ (Figure 1b). This situation might be typical, for example, for the bottom of an attenuative reservoir. Because the angle ξ is determined by the medium properties along the whole raypath, the imaginary part $\mathbf{k}^I$ of the wave vector might even deviate from the vertical incidence plane. However, for simplicity we assume that this deviation can be ignored.

For a nonzero angle ξ, the real and imaginary parts of the wave vector $\tilde{\mathbf{k}}$ are not parallel, and the Christoffel equation becomes

$$(\tilde{a}_{ijkl}\tilde{k}_i\tilde{k}_l - \omega\delta_{jk})\tilde{u}_j = 0. \tag{22}$$

Although the perturbation analysis of Jech and Pšenčík (1989) is not strictly valid for equation 22, it remains sufficiently accurate for moderate values of ξ, if the quality factor is not uncommonly small (Zhu and Tsvankin, 2006). Therefore, the formulation of Vavryčuk and Pšenčík (1998) and Jílek (2002a, 2002b) can be applied in a straightforward way to linearize the reflection coefficient for an incident wave with a nonzero ξ. The numerical results below confirm that this approach yields an accurate approximation for most plausible attenuative models.

PP-wave reflection coefficient

The linearized PP-wave reflection coefficient $R_{\text{PP}}^{\text{IH}}$ for arbitrarily anisotropic media and for the incident wave with $\xi \neq 0°$ represents a linear function f_0 of the following parameters:

$$R_{\text{PP}}^{\text{IH}} = f_0(\Delta\rho/\rho^0, \tilde{V}_{\text{P0}}, \tilde{V}_{\text{S0}}, \Delta\tilde{a}_{11}, \Delta\tilde{a}_{13}, \Delta\tilde{a}_{15},$$
$$\Delta\tilde{a}_{33}, \Delta\tilde{a}_{35}, \Delta\tilde{a}_{55}, \theta, \xi), \tag{23}$$

where the superscript IH (inhomogeneous) indicates that the incident wave has a nonzero inhomogeneity angle. Because of the complicated form of f_0, it is not shown explicitly in the paper. The reflection coefficient in equation 23 depends on three additional stiffness contrasts ($\Delta\tilde{a}_{11}$, $\Delta\tilde{a}_{15}$, and $\Delta\tilde{a}_{35}$) compared to the reflection coefficient for $\xi = 0°$ (equation 14).

For VTI media, the perturbation result 23 reduces to

$$R_{\text{PP}}^{\text{IH}} = R_{\text{PP}}^{\text{IH}}(0) + B_{\text{PP}}^{\text{IH}}\sin\theta + G_{\text{PP}}^{\text{IH}}\sin^2\theta, \tag{24}$$

where

$$R_{\text{PP}}^{\text{IH}}(0) = R_{\text{PP}}^{\text{H}}(0) + \frac{\sin^2\xi}{4Q_{\text{P0}}}f_5, \tag{25}$$

$$B_{\text{PP}}^{\text{IH}} = \frac{-i\sin\xi}{Q_{\text{P0}}}f_6, \tag{26}$$
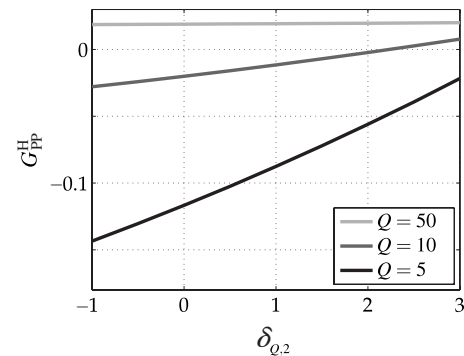
and

Figure 4. PP-wave AVO gradient as a function of the attenuation-anisotropy parameter $\delta_{Q,2}$ in the reflecting half-space. The gradient is estimated numerically as the initial slope of the exact PP-wave reflection coefficient computed as a function of $\sin^2\theta$. The model is similar to that in Figure 3, but the attenuation in the reflecting oil sand is anisotropic (Table 1). The curves correspond to different Q-values in the sand ($Q = Q_{\text{P0,2}} = 2Q_{\text{S0,2}}$).

$$G_{PP}^{IH} = G_{PP}^{H} + \frac{i \sin^2 \xi}{8 Q_{P0}} f_7. \qquad (27)$$

Here, $R_{PP}^{H}(0)$ and G_{PP}^{H} are the solutions for $\xi = 0°$ (superscript H) given by equations 16 and 17, respectively, and f_5, f_6, and f_7 are linear functions listed in Appendix A.

As illustrated by Figure 5, equation 24 remains accurate for moderate inhomogeneity angles reaching 30°. Even for $Q = 2.5$ and $\xi = 30°$ (Figure 5i), approximation 24 deviates from the exact reflection coefficient by less than 10%.

In contrast to the conventional AVO equation for pure (nonconverted) waves, which represents an even function of θ (e.g., equation 15), equation 24 includes the $\sin \theta$-term. Therefore, the contribution of the inhomogeneity angle makes the basic equation of conventional PP-wave AVO analysis inadequate, which could have significant implications for AVO inversion and interpretation.

However, because the angle ξ is associated with the terms f_5, f_6,

and f_7, which are scaled by $1/Q_{P0}$, its influence becomes pronounced only in strongly attenuative media. Indeed, the variation of the inhomogeneity angle from 0° to 50° does not significantly change the exact reflection coefficient for $Q \geq 10$ (Figure 6a and b). Only when $Q = 5$ and the inhomogeneity angle exceeds 30°, the contribution of ξ to the reflection coefficient (in particular, to the term B_{PP}^{IH}) becomes substantial (Figure 6c).

The asymmetry of the reflection coefficient with respect to $\theta = 0°$ (Figure 6b and c), which increases with the inhomogeneity angle, is explained in Figure 7. In our modeling, the inhomogeneity angle of the incident wave is fixed (i.e., it is independent of θ), which implies that the imaginary part $\mathbf{k}^I$ of the wave vector makes different angles with the vertical for the incidence angles θ and $-\theta$. As a result, the reflection coefficient for positive incidence angles differs from that for negative angles.

In reality, it is unlikely for the incident wave to have a constant inhomogeneity angle for a wide range of θ. A more plausible scenario
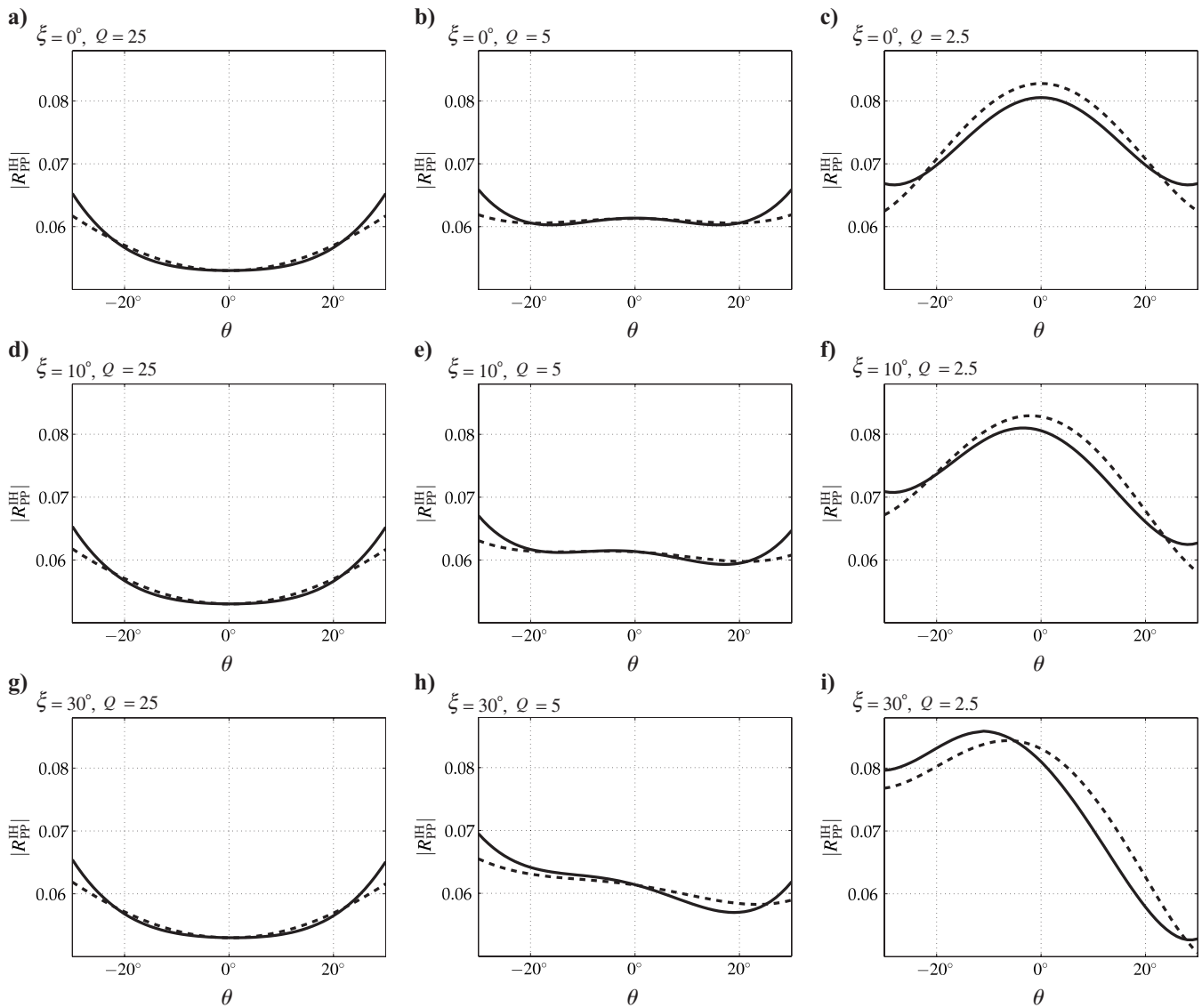

Figure 5. Magnitude of the exact (solid lines) and approximate (dashed lines, equation 24) PP-wave reflection coefficient at a VTI/isotropic interface for different inhomogeneity angles. The quality factors are (a) $Q = 50$; (b) $Q = 10$; and (c) $Q = 5$, where $Q = Q_{P0,1} = 2Q_{S0,1} = Q_{P0,2}/2 = Q_{S0,2}$; the other model parameters are listed in Table 1.
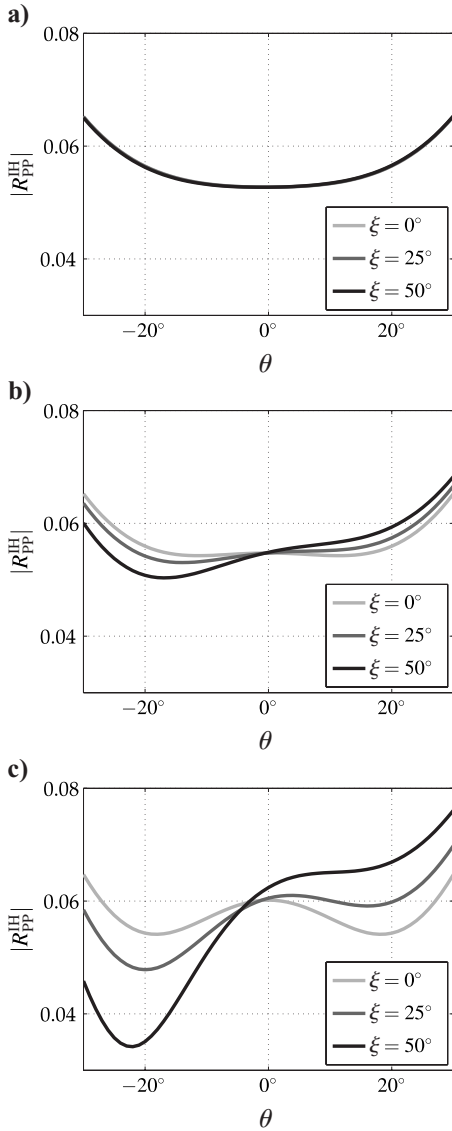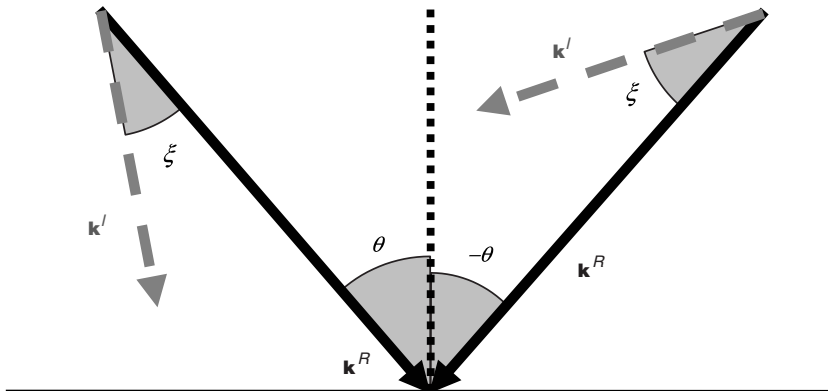
a)

b)

c)

Figure 6. Magnitude of the exact PP-wave reflection coefficient at a VTI/isotropic interface for different inhomogeneity angles. The quality factors are (a) $Q = 50$; (b) $Q = 10$; and (c) $Q = 5$, where $Q = Q_{P0,1} = 2Q_{S0,1} = 2Q_{P0,2} = 4Q_{S0,2}$. The other model parameters are listed in Table 1.

Figure 7. PP-wave reflection coefficient might become asymmetric with respect to $\theta = 0°$ for a nonzero inhomogeneity angle ξ. As before, $\mathbf{k}^R$ and $\mathbf{k}^I$ are the real and imaginary parts, respectively, of the wave vector of the incident P-wave.

is depicted in Figure 8a. The model includes an attenuative reservoir beneath a purely elastic cap rock. Because the cap rock is nonattenuative, the wave incident upon the reservoir has a real wave vector. According to Snell's law, the horizontal slowness (and the horizontal component of the wave vector) must be preserved during reflection and transmission. Therefore, the imaginary part $\mathbf{k}^I$ of the wave vector in the reservoir cannot have a horizontal component, and the inhomogeneity angle of the transmitted wave is equal to the transmission angle θ_T (Figure 8a). For the reflection from the bottom of the reservoir, θ_T becomes the incidence angle. Therefore, the vector $\mathbf{k}^I$ for both positive and negative incidence angles remains vertical (i.e., the wave vector as a whole is symmetric with respect to the reflector normal), and the PP-wave reflection coefficient is an even function of θ (Figure 8b, gray line). However, for more complicated overburden models, the inhomogeneity angle can be different from the incidence angle, which makes the reflection coefficient asymmetric with respect to θ (Figure 8b, black line; $\xi = 50°$ was held constant).

PS-wave reflection coefficient

As is the case for PP-waves, the influence of the inhomogeneity angle of the incident P-wave changes the conventional PS-wave AVO equation. The linearized PS-wave coefficient for $\xi \neq 0$ becomes

$$R_{PS}^{IH} = R_{PS}^{IH}(0) + B_{PS}^{IH} \sin\theta + G_{PS}^{IH} \sin^2\theta, \quad (28)$$

where

$$R_{PS}^{IH}(0) = i\frac{\sin\xi}{Q_{P0}}f_8, \quad (29)$$

$$B_{PS}^{IH} = B_{PS}^{H}, \quad (30)$$

and

$$G_{PS}^{IH} = -i\frac{\sin\xi}{Q_{P0}}f_9. \quad (31)$$

Equations 28–31 do not include cubic and higher order terms in $\sin\theta$ and $\sin\xi$. The term B_{PS}^{H} is the PS-wave AVO gradient for an incident wave with a zero inhomogeneity angle (equation 20), and the terms f_8 and f_9 are linear combinations of the parameter contrasts across the interface (Appendix A).

Equation 28 is different from equation 19 for $\xi = 0°$, in which only the coefficients of odd powers in $\sin\theta$ are nonzero (i.e., the reflection coefficient is an odd function of θ). The deviation of equation 28 from the conventional PS-wave AVO equation is illustrated in Figure 9, where the absolute value of the PS-wave reflection coefficient in strongly attenuative media ($Q = 2.5$) for $\xi = 50°$ is visibly asymmetric with respect to $\theta = 0°$. Whereas the coefficient R_{PS}^{IH} for $Q = 50$ almost coincides with that for a purely elastic medium, the influence of attenuation and the inhomogeneity angle becomes pronounced for low values of Q.

Because the linearized AVO gradient B_{PS}^{IH} (equation 30) does not depend on ξ, the inhomogeneity angle has a greater influence on $R_{PS}^{IH}(0)$ and G_{PS}^{IH} than on B_{PS}^{IH}. For a zero inhomogeneity angle of the in-

a)

Elastic cap rock
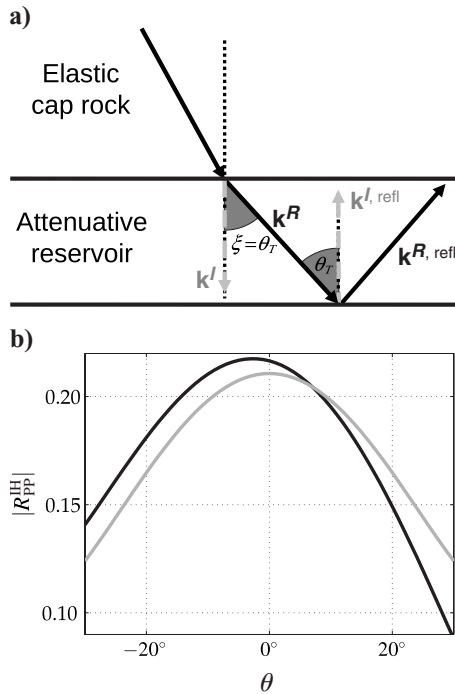
Attenuative reservoir

b)

Figure 8. (a) The vectors of the incident and reflected waves in an attenuative layer (reservoir) overlaid by a purely elastic medium (cap rock). The inhomogeneity angle ξ of the wave transmitted through the top of the reservoir is equal to the transmission angle θ_T. The vectors $\mathbf{k}^{R,refl}$ and $\mathbf{k}^{I,refl}$ are the real and imaginary components, respectively, of the wave vector for the reflection from the bottom of the reservoir. (b) Magnitude of the exact PP-wave reflection coefficient from the reservoir bottom for $\xi = \theta_T$ (gray line) and for a constant inhomogeneity angle $\xi = 50°$ (black line). The model parameters are listed in Table 1.
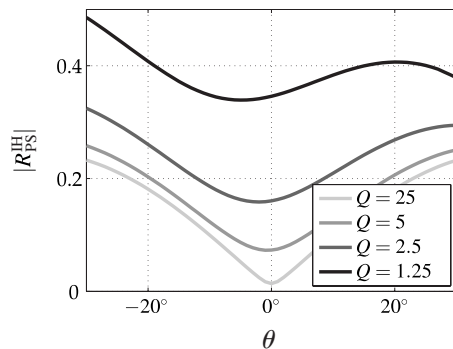

Figure 9. Magnitude of the exact PS-wave reflection coefficient at an isotropic/VTI interface for a nonzero inhomogeneity angle ($\xi = 50°$) of the incident P-wave and variable quality factor $Q = Q_{P0,1} = 2Q_{S0,1} = Q_{P0,2}/2 = Q_{S0,2}$. The other model parameters are listed in Table 1.

cident wave, $R_{PS}^{IH}(0)$ and G_{PS}^{IH} vanish and equation 28 reduces to the term proportional to $\sin\theta$ in equation 19.

For $\xi \neq 0°$ and small Q-values, the magnitude of the normal-incidence PS-wave reflection coefficient $R_{PS}^{IH}(0)$ can be substantial (Figure 9). A nonzero inhomogeneity angle of the vertically traveling P-wave makes its wave vector asymmetric with respect to the reflector normal, which generates the PS conversion. Note that generation of reflected or transmitted PS-waves at normal incidence also can be caused by such factors as lateral heterogeneity, the deviation of the reflector from the symmetry planes of the model (Behura and Tsvankin, 2006), and the influence of additional terms of the ray-series expansion on point-source radiation (Tsvankin, 1995). Here, however, the model is composed of homogeneous VTI half-spaces with a common horizontal symmetry plane, and we consider only plane-wave reflection coefficients.

DISCUSSION

The plane-wave reflection coefficients analyzed here are derived for plane interfaces and, therefore, break down in the presence of significant wavefront and/or reflector curvature (van der Baan and Smit, 2006; Ayzenberg et al., 2009). Reflections from curved interfaces can be analyzed by using so-called "effective reflection coefficients" (ERC), extended to anisotropic media by Ayzenberg et al. (2009). Plane-wave reflection coefficients often are incorporated into the geometrical-seismics approximation to describe wavefields generated by point sources. Geometrical seismics, however, loses accuracy for near- and postcritical incidence angles and for source/receiver locations near the reflector. If the interface is plane, the exact scattered wavefields can be modeled using Weyl-type integrals, which include plane-wave reflection/transmission coefficients (Tsvankin, 1995).

In contrast to most previous publications, our formalism considers the inhomogeneity angle ξ of the incident wave. As demonstrated above, reflection coefficients of both PP- and PS-waves become sensitive to the angle ξ only when it is relatively large and the medium is highly attenuative. This result facilitates AVO analysis in attenuative media because the inhomogeneity angle is extremely difficult to evaluate from seismic data. Indeed, the group attenuation coefficient (i.e., the attenuation along the raypath) measured from seismic amplitudes is independent of ξ for a wide range of small and moderate inhomogeneity angles (Behura and Tsvankin, 2009). Potentially, the inhomogeneity angle can be estimated from the reflection coefficient provided a priori information about the parameter contrasts is available and ξ is sufficiently large. However, the increase in the group attenuation coefficient for large values of ξ (Behura and Tsvankin, 2009) reduces the reflection amplitude and makes AVO analysis less reliable.

The stiffness tensor in attenuative media is not only complex, but also varies with frequency, which makes velocity, normalized attenuation coefficient, and other quantities frequency-dependent. Our analytic expressions are derived for a fixed frequency of the harmonic plane wave and can be applied to arbitrarily dispersive models by treating the stiffnesses or Thomsen-style parameters as functions of frequency.

CONCLUSIONS

To analyze PP- and PS-wave reflection coefficients in attenuative anisotropic media, we developed linearized approximations using perturbation theory. For an incident P-wave with a zero inhomogeneity angle, the form of the linearized PP- and PS-wave reflection coefficients in arbitrarily anisotropic media is the same as in purely elastic models, but all terms become complex. The general solutions were simplified for VTI symmetry to obtain simple closed-form expressions in Thomsen-style notation.

Both analytic and numerical results show that only in the presence of strong attenuation ($Q < 10$) does the contribution of the imaginary part of the stiffness tensor (which is responsible for attenuation) become comparable to that of the real part. In particular, the influence of the attenuation-anisotropy parameters ϵ_Q and δ_Q on the PP-wave reflection coefficient typically is much weaker than that of the velocity-anisotropy parameters ε and δ. As expected from the parameter definitions, the PP-wave AVO gradient in attenuative media includes δ_Q, and the wide-angle reflection coefficient also depends on ε_Q. However, the largest attenuation-related terms in the reflection coefficients for both PP- and PS-waves are proportional to the contrasts in the normalized symmetry-direction attenuation coefficients $\mathcal{A}_{P0}$ and $\mathcal{A}_{S0}$ because the contrasts in the attenuation-anisotropy parameters are scaled by the inverse quality factor $1/Q_{P0}$. Therefore, the contribution of ε_Q and δ_Q becomes significant only for models with uncommonly high attenuation ($Q < 10$), such as heavy-oil-saturated rocks.

If the incident wave has a nonzero inhomogeneity angle ξ, the form of the linearized reflection coefficients is different from the conventional AVO expression. In particular, the PP-wave reflection coefficient no longer is an even function of the incidence angle θ and includes a term proportional to $\sin\theta$. Likewise, when $\xi \neq 0°$, the normal-incidence PS-wave reflection coefficient (i.e., the AVO intercept) does not vanish and might even attain values comparable to the AVO intercept for the PP reflection. However, the inhomogeneity angle makes a substantial contribution to the AVO response only for strongly attenuative media.

Despite the presence of attenuation-related terms, our linearized AVO equations have an easily interpretable form that provides useful physical insight into the reflectivity of anisotropic attenuative media. Their application can help avoid errors in AVO analysis and, potentially, invert prestack reflection amplitudes for the attenuation parameters.

ACKNOWLEDGMENTS

APPENDIX A

LINEAR FUNCTIONS IN THE APPROXIMATE REFLECTION COEFFICIENTS

Here, we give explicit expressions for the linear functions f_i in the approximate equations for the reflection coefficients.

The functions f_1, f_2, f_3, and f_4 in equations 20 and 21 have the form

$$f_1 = \frac{1}{2g}\frac{\Delta\rho}{\rho_0} + \frac{1}{g}\frac{\Delta V_{S0}}{V_{S0}} + \frac{g}{4(1+g)^2}\Delta\delta + \frac{i}{g}\Delta\mathcal{A}_{S0}$$
$$+ \frac{g}{4(1+g)}\Delta\delta_Q, \tag{A-1}$$

$$f_2 = \frac{1}{2g}\frac{\Delta\rho}{\rho_0} + \frac{1}{g}\frac{\Delta V_{S0}}{V_{S0}} + \frac{g}{4(1+g)^2}\Delta\delta + \frac{i}{g}\Delta\mathcal{A}_{S0}, \tag{A-2}$$

$$f_3 = \frac{3+g}{2g^2}\frac{\Delta\rho}{\rho_0} + \frac{4+g}{g^2}\frac{\Delta V_{S0}}{V_{S0}} - \frac{g}{(1+g)^2}\Delta\varepsilon$$
$$+ \frac{5g}{4(1+g)^2}\Delta\delta + i\frac{4+g}{g^2}\Delta\mathcal{A}_{S0} - \frac{g}{(1+g)^2}\Delta\varepsilon_Q$$
$$+ \frac{4g-1}{4(1+g)}\Delta\delta_Q, \tag{A-3}$$

and

$$f_4 = \frac{3+g}{2g^2}\frac{\Delta\rho}{\rho_0} + \frac{4+g}{g^2}\frac{\Delta V_{S0}}{V_{S0}} - \frac{g}{(1+g)^2}\Delta\varepsilon$$
$$+ \frac{5g}{4(1+g)^2}\Delta\delta + i\frac{1}{g^2}\Delta\mathcal{A}_{S0}, \tag{A-4}$$

where $g \equiv V_{P0}/V_{S0}$.

The functions f_5, f_6, and f_7 in equations 25–27 are given by

$$f_5 = -i\frac{\Delta V_{P0}}{V_{P0}} + \Delta\mathcal{A}_{P0}, \tag{A-5}$$

$$f_6 = \frac{-2}{g^2}\frac{\Delta\rho}{\rho_0} + \frac{\Delta V_{P0}}{2V_{P0}} - \frac{4}{g^2}\frac{\Delta V_{S0}}{V_{S0}} + \frac{\Delta\delta}{2}$$
$$+ i\left(\frac{\Delta\mathcal{A}_{P0}}{2} - \frac{4\Delta\mathcal{A}_{S0}}{g^2}\right), \tag{A-6}$$

and

$$f_7 = \left(1 + \frac{1}{g^2}\right)\frac{\Delta V_{P0}}{V_{P0}} - \Delta\delta + i\left(1 + \frac{1}{g^2}\right)\Delta\mathcal{A}_{P0}. \tag{A-7}$$

Finally, for the functions f_8 and f_9 in equations 29 and 31, we have

$$f_8 = \frac{2+g}{4g}\frac{\Delta\rho}{\rho_0} + \frac{\Delta V_{S0}}{gV_{S0}} - \frac{g}{4(1+g)}\Delta\delta + \frac{i}{g}\Delta\mathcal{A}_{S0}, \tag{A-8}$$

and

$$f_9 = \frac{9+8g+g^2}{8g^2}\frac{\Delta\rho}{\rho_0} + \frac{3+2g}{g^2}\frac{\Delta V_{S0}}{V_{S0}} + \frac{3-13g}{8(1+g)}\Delta\delta$$
$$+ \frac{3g}{2(1+g)}\Delta\varepsilon + i\frac{3+2g}{g^2}\Delta\mathcal{A}_{S0}. \tag{A-9}$$

REFERENCES

Arts, R. J., and P. N. J. Rasolofosaon, 1992, Approximation of velocity and attenuation in general anisotropic rocks: 62nd Annual International Meeting, SEG, Expanded Abstracts, 640–643.

Ayzenberg, M., I. Tsvankin, A. Aizenberg, and B. Ursin, 2009, Effective reflection coefficients for curved interfaces in transversely isotropic media: Geophysics, this issue.

Behura, J., M. Batzle, and R. Hofmann, 2006, Shear properties of oil shales: 76th Annual International Meeting, SEG, Expanded Abstracts, 1973–1977.

Behura, J., M. Batzle, R. Hofmann, and J. Dorgan, 2007, Heavy oils: Their shear story: Geophysics, **72**, no. 5, E175–E183.

Behura, J., and I. Tsvankin, 2006, Small-angle AVO response of PS-waves in tilted transversely isotropic media: Geophysics, **71**, no. 5, C69–C79.

——Behura, J., and I. Tsvankin, 2009, Role of the inhomogeneity angle in anisotropic attenuation analysis: Geophysics, this issue.

Carcione, J. M., 2007, Wave fields in real media: Wave propagation in anisotropic, anelastic, porous and electromagnetic media, 2nd ed.: Elsevier Science.

Hauge, P. S., 1981, Measurements of attenuation from vertical seismic profiles: Geophysics, **46**, 1548–1558.

Hearn, D. J., and E. S. Krebes, 1990, On computing ray-synthetic seismograms for anelastic media using complex rays: Geophysics, **55**, 422–432.

Hedlin, K., L. Mewhort, and G. Margrave, 2001, Delineation of steam flood using seismic attenuation: 71st Annual International Meeting, SEG, Expanded Abstracts, 1572–1575.

Hosten, B., M. Deschamps, and B. R. Tittmann, 1987, Inhomogeneous wave generation and propagation in lossy anisotropic solids — Application to the characterization of viscoelastic composite materials: Journal of the Acoustical Society of America, **82**, 1763–1770.

Jech, J., and I. Pšenčík, 1989, First-order perturbation method for anisotropic media: Geophysical Journal International, **99**, 369–376.

Jílek, P., 2002a, Converted PS-wave reflection coefficients in weakly anisotropic media: Pure and Applied Geophysics, **159**, 1527–1562.

———, 2002b, Modeling and inversion of converted-wave reflection coefficients in anisotropic media: A tool for quantitative AVO analysis: Ph.D. thesis, Colorado School of Mines.

Krebes, E. S., 1983, The viscoelastic reflection/transmission problem: Two special cases: Bulletin of Seismological Society of America, **73**, 1673–1683.

Liu, E., S. Crampin, J. H. Queen, and W. D. Rizer, 1993, Velocity and attenuation anisotropy caused by microcracks and microfractures in a multiazimuth reverse VSP: Canadian Journal of Exploration Geophysics, **29**, 177–188.

Luh, P. C., 1988, Wavelet dispersion and bright spot detection: 58th Annual International Meeting, SEG, Expanded Abstracts, 1217–1220.

Lynn, H. B., D. Campagna, K. M. Simon, and W. E. Beckham, 1999, Relationship of P-wave seismic attributes, azimuthal anisotropy, and commercial gas pay in 3-D P-wave multiazimuth data, Rulison Field, Piceance Basin, Colorado: Geophysics, **64**, 1293–1311.

Maultzsch, S., M. Chapman, E. Liu, and X. Y. Li, 2003, Modeling frequency-dependent seismic anisotropy in fluid-saturated rock with aligned fractures: Implication of fracture size estimation from anisotropic measurements: Geophysical Prospecting, **51**, 381–392.

Nechtschein, S., and F. Hron, 1997, Effects of anelasticity on reflection and transmission coefficients: Geophysical Prospecting, **45**, 775–793.

Prasad, M., and A. Nur, 2003, Velocity and attenuation anisotropy in reservoir rocks: 73rd Annual International Meeting, SEG, Expanded Abstracts, 1652–1655.

Rüger, A., 2002, Reflection coefficients and azimuthal AVO analysis in anisotropic media: SEG.

Samec, P., J. P. Blangy, and A. Nur, 1990, Effect of viscoelasticity and anisotropy on amplitude-versus-offset interpretation: 60th Annual International Meeting, SEG, Expanded Abstracts, 1479–1482.

Schmitt, D. R., 1999, Seismic attributes for monitoring of a shallow heated heavy oil reservoir: A case study: Geophysics, **64**, 368–377.

Sidler, R., and J. M. Carcione, 2007, Wave reflection at an anelastic transversely isotropic ocean bottom: Geophysics, **72**, no. 5, SM139–SM146.

Stovas, A., and B. Ursin, 2003, Reflection and transmission responses of layered transversely isotropic viscoelastic media: Geophysical Prospecting, **51**, 447–477.

Tao, G., and M. S. King, 1990, Shear-wave velocity and Q anisotropy in rocks: A laboratory study: International Journal of Rock Mechanics and Mining Science & Geomechanics Abstracts, **27**, 353–361.

Tsvankin, I., 1995, Seismic wavefields in layered isotropic media: Samizdat Press.

Ursin, B., and A. Stovas, 2002, Reflection and transmission responses of a layered isotropic viscoelastic medium: Geophysics, **67**, 307–323.

van der Baan, M., and D. Smit, 2006, Amplitude analysis of isotropic P-wave reflections: Geophysics, **71**, no. 6, C93–C103.

Vasconcelos, I., and E. Jenner, 2005, Estimation of azimuthally varying attenuation from wide-azimuth P-wave data: 75th Annual International Meeting, SEG, Expanded Abstracts, 123–126.

Vavryčuk, V., and I. Pšenčík, 1998, PP-wave reflection coefficients in weakly anisotropic elastic media: Geophysics, **63**, 2129–2141.

Winkler, K. W., and A. Nur, 1982, Seismic attenuation: Effects of pore fluids and frictional-sliding: Geophysics, **47**, 1–15.

Zhu, Y., and I. Tsvankin, 2006, Plane-wave propagation in attenuative transversely isotropic media: Geophysics, **71**, no. 2, T17–T30.

Zhu, Y., I. Tsvankin, P. Dewangan, and K. van Wijk, 2007, Physical modeling and analysis of P-wave attenuation anisotropy in transversely isotropic media: Geophysics, **72**, no. 1, D1–D7.